Images displaying a number of structures and techniques on biophysics studies into macromolecules referenced as 'Dr Fuller'.

Contributors

Fuller, Watson, b.1935

Publication/Creation

January 1967

Persistent URL

https://wellcomecollection.org/works/ndb74srw

License and attribution

wellcome collection

Wellcome Collection
183 Euston Road
London NW1 2BE UK
T +44 (0)20 7611 8722
E library@wellcomecollection.org
https://wellcomecollection.org

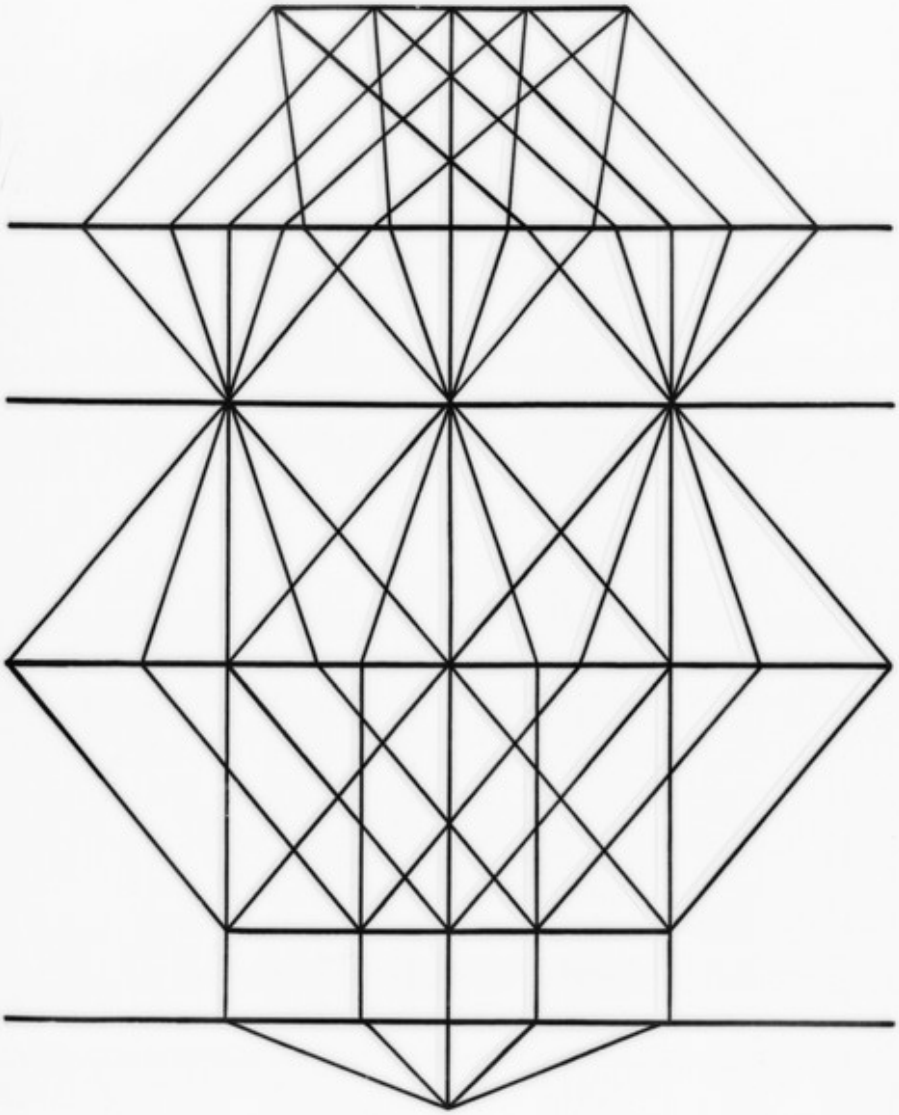

7896

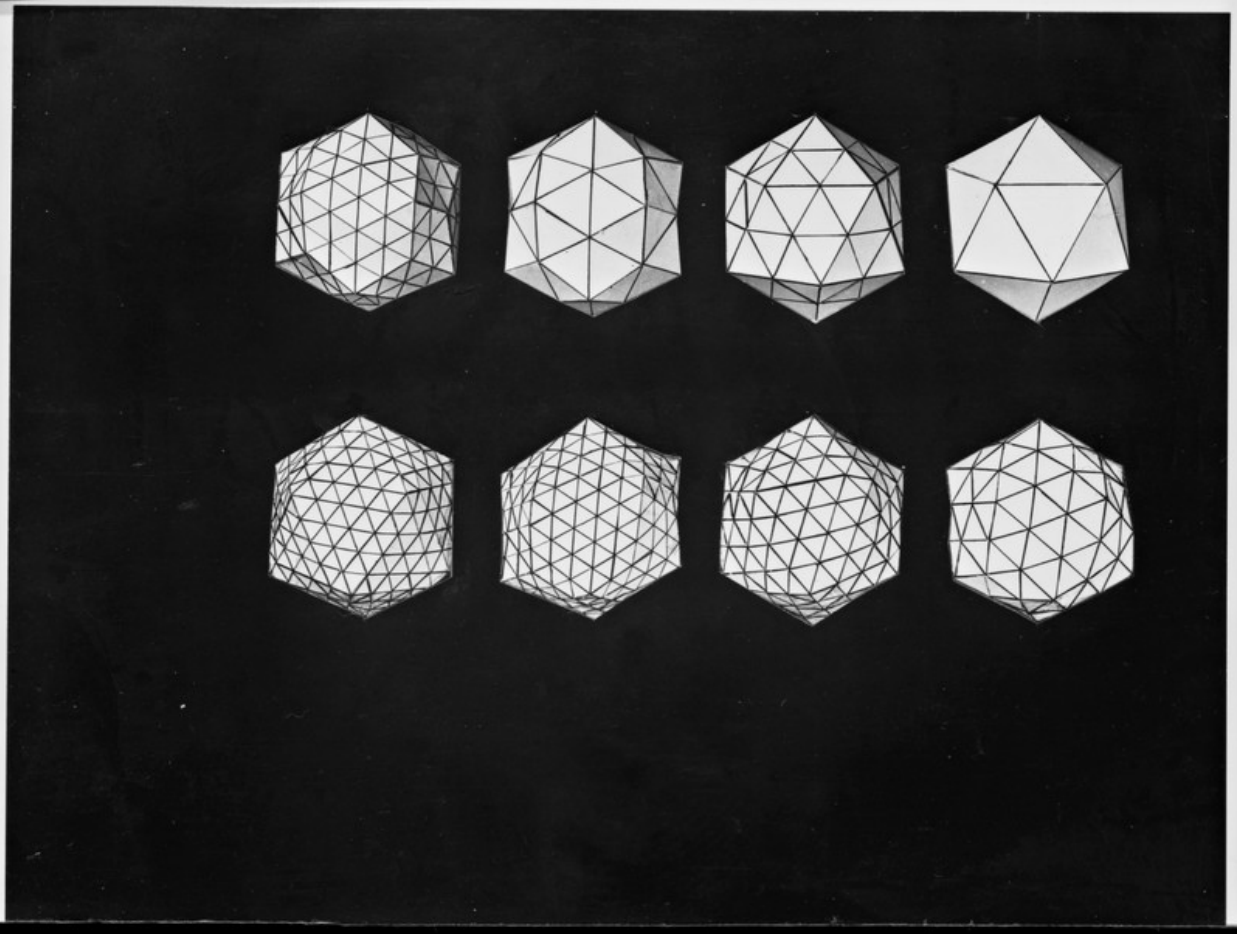

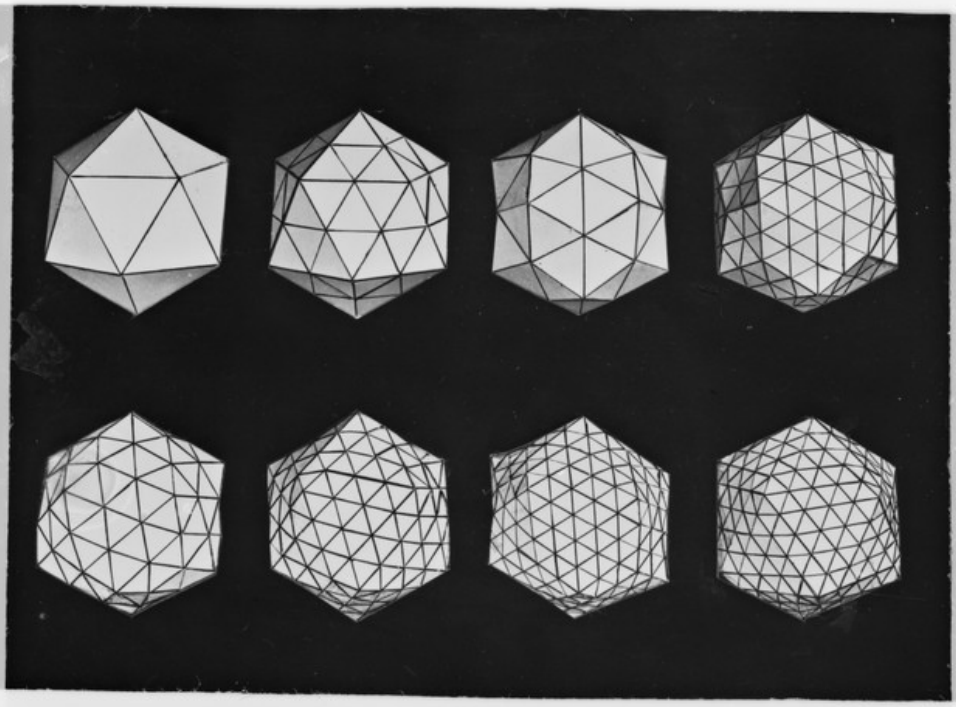

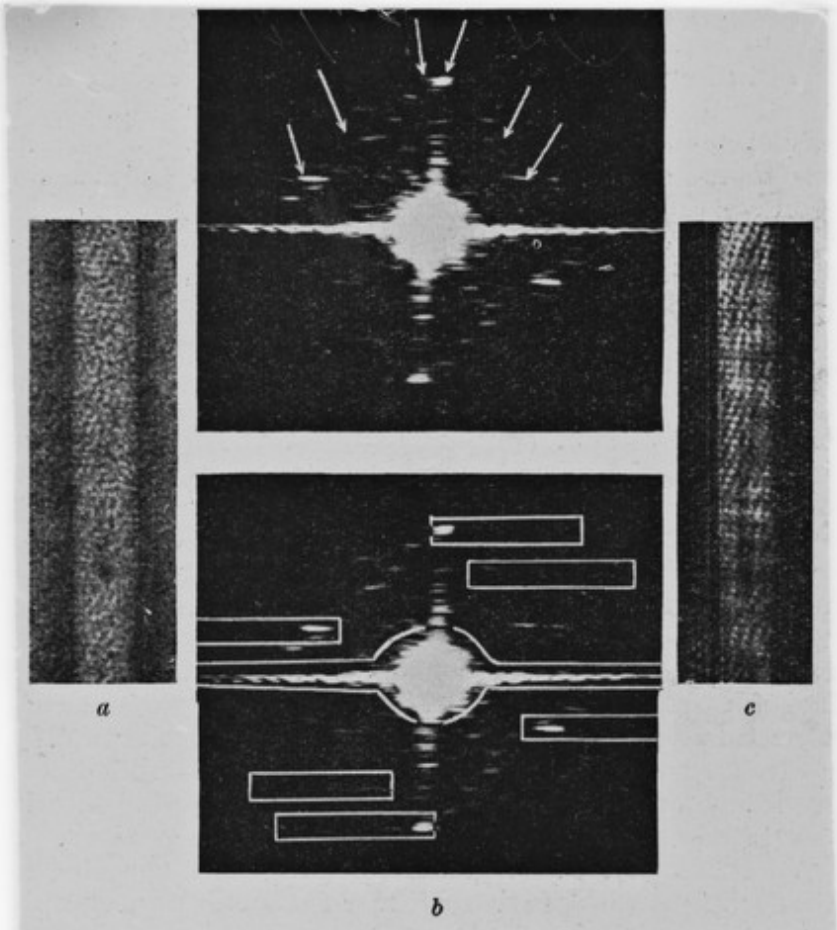

a, Electron micrograph of a negatively stained particle of tobacco mosaic virus (ref. 7). Patches of stain are visible in the central hole. **b**, Diffraction pattern of **a** (× 1·6). The arrows indicate the position of the spots which are constant features of the diffraction patterns of TMV images (ref. 4). The other spots do not recur in all patterns and are attributed to irregularities in the staining and non-systematic perturbations in the particle structure. The asymmetry between the left and right sides of the 69Å and 23Å layer lines shows that in this particle the contrast is unequally developed on the two sides. That is to say, the image is largely one-sided. **c**, Filtered image of **a**, admitting only the diffracted rays shown boxed in the lower photograph in **b** (× 330,000).

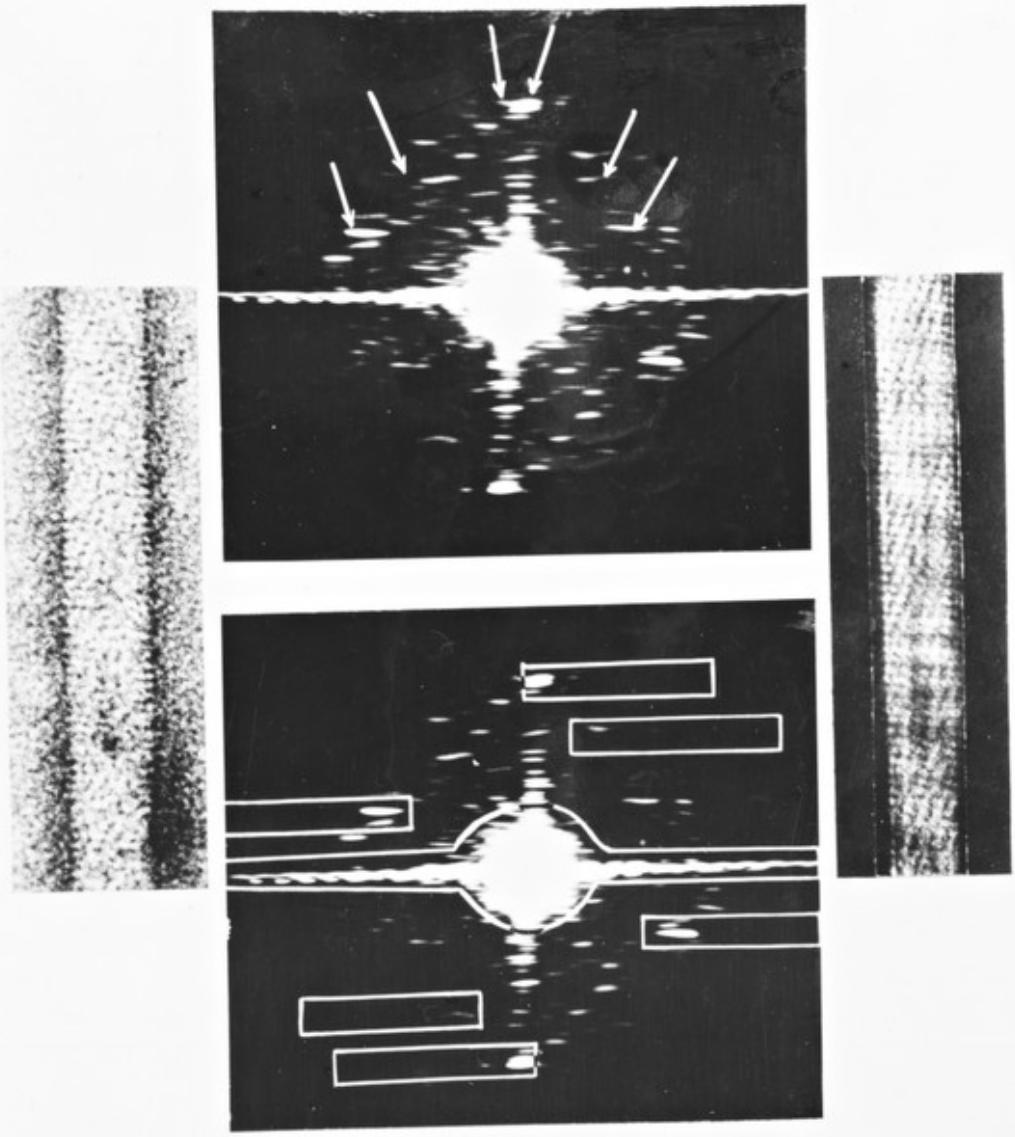

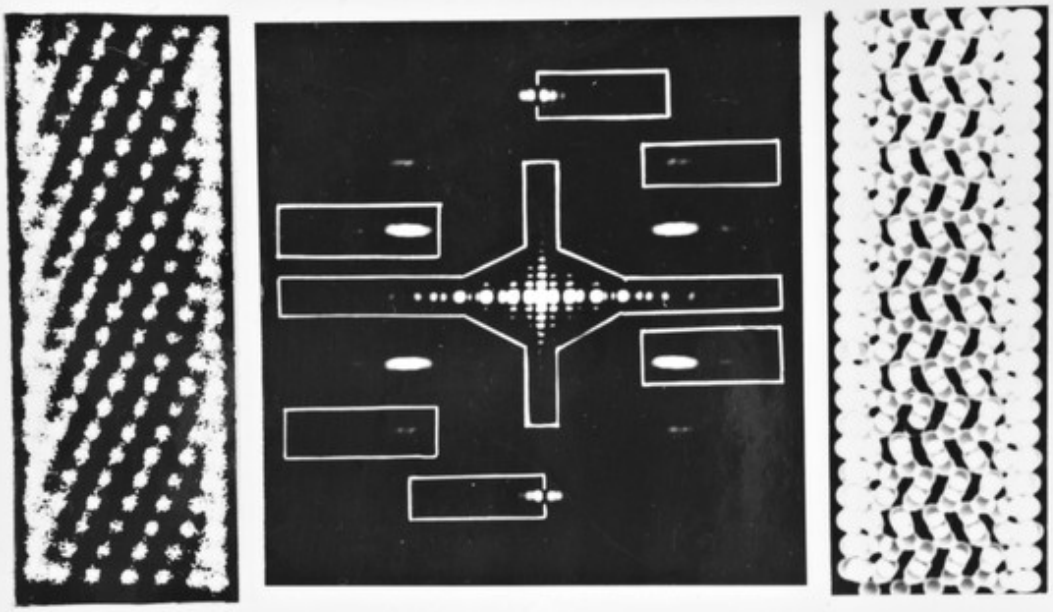

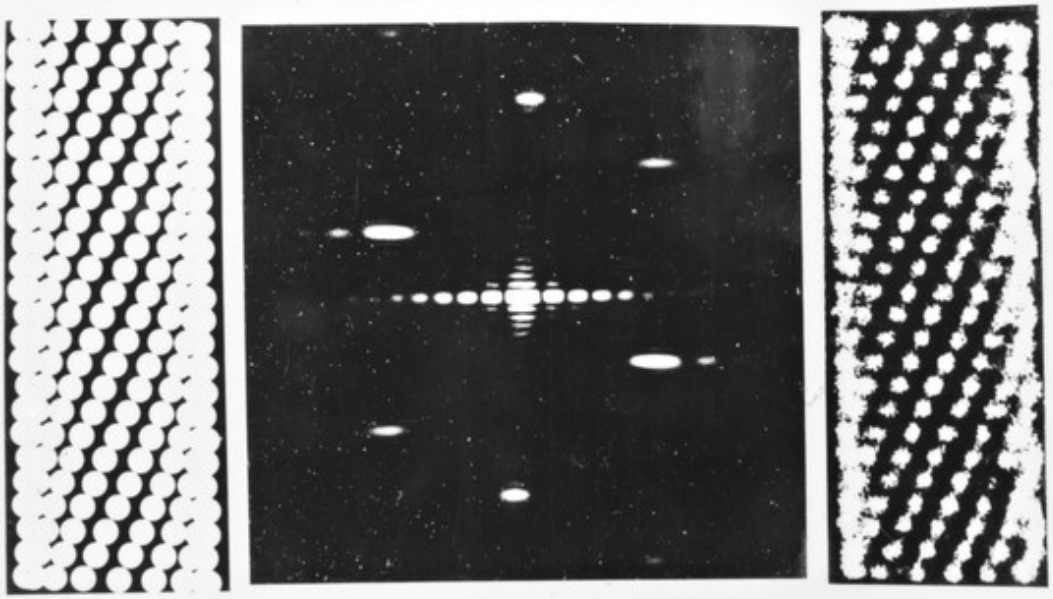

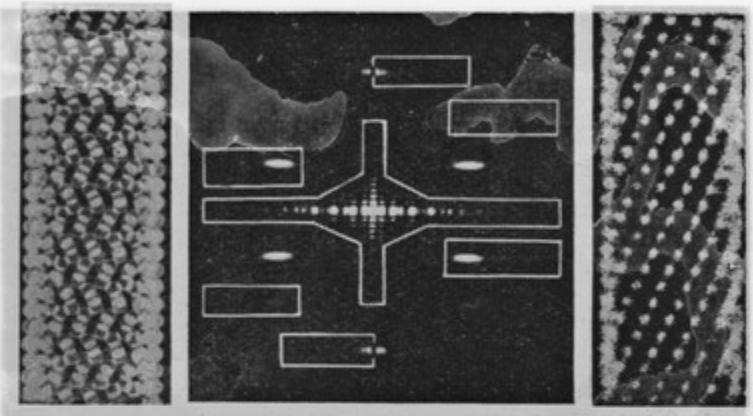

a *b* *c*

a, Positive replica of a photographic transparency representing the orthogonal projection of a helical structure on to a plane through the axis. The parameters of the structure have been chosen so that they are the same as those of tobacco mosaic virus at a radius of 100 Å. *b*, Fraunhofer diffraction pattern of *a* (× 1·5). *c*, Filtered image of *a*, obtained by admitting through the imaging lens only the diffracted rays indicated by the boxes in *b*.

a *b* *c*

a, Projection of one side only of the helical structure of Fig. 2*a*. *b*, Diffraction pattern of *a* (× 1·5). Note that the principal diffraction spots lie approximately at the vertices of a lattice. *c*, Image of *a* without any filtering. The loss of quality arises from imperfections in the optical system.

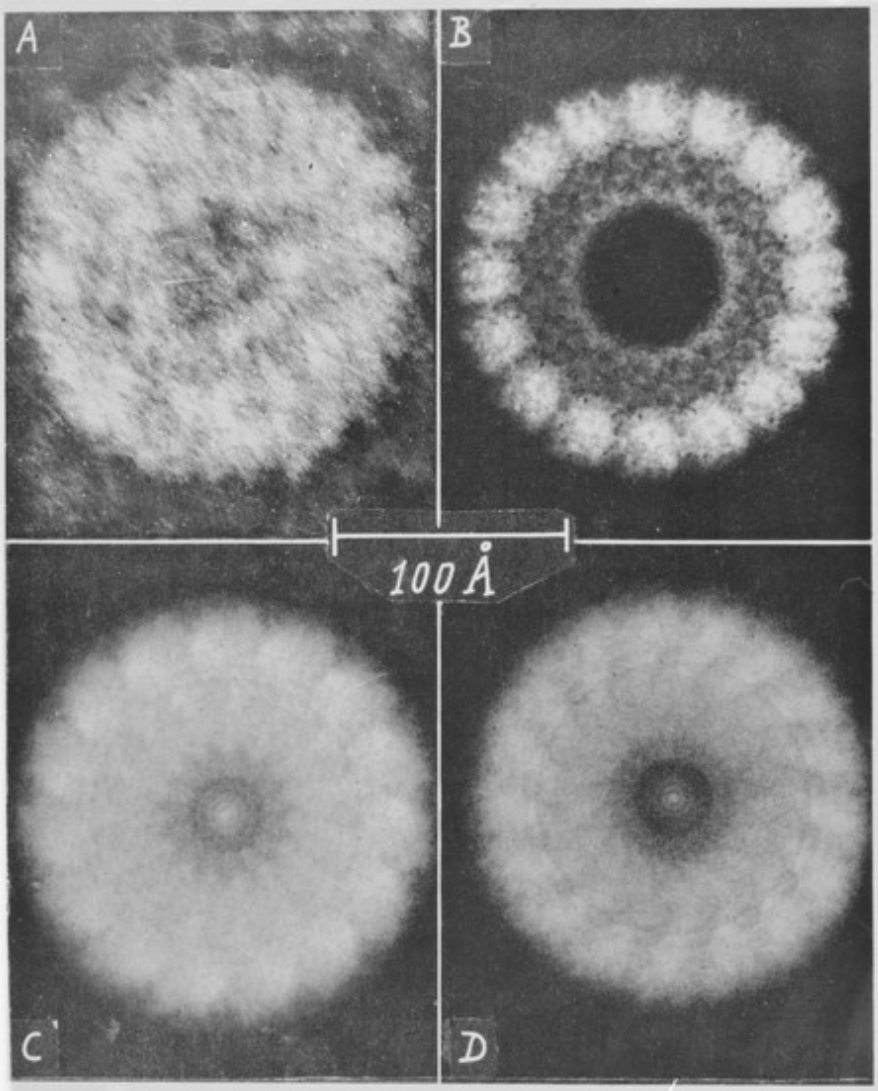

Tobacco mosaic virus X-protein in the stacked disk configuration as seen "end-on." (A) Original electron micrograph. (B) Rotated $n = 16$. (C) Rotated $n = 15$. (D) Rotated $n = 17$.

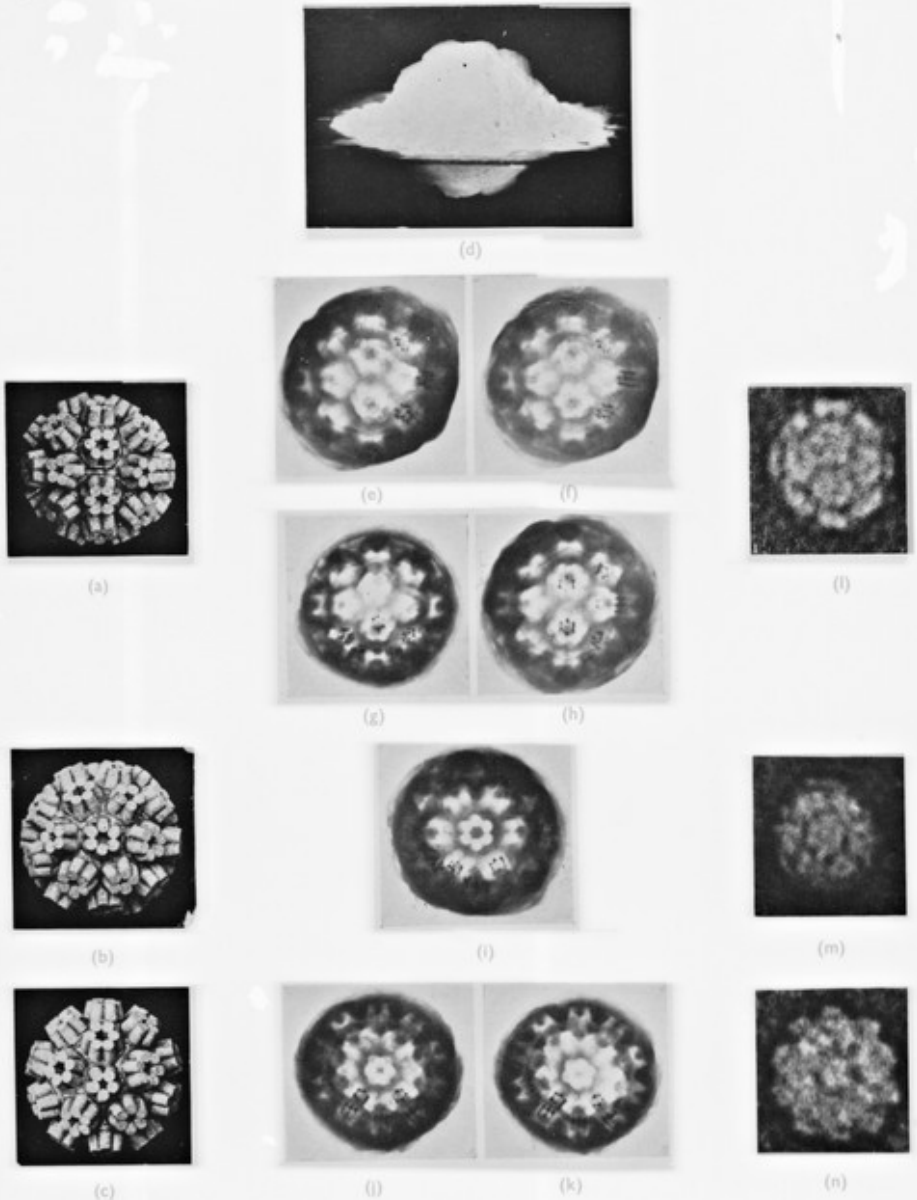

PLATE III. (a), (b) and (c) Photographs of a cork model of turnip yellow mosaic virus taken down 2-, 3- and 5-fold axes, respectively.

(d) The cork model embedded in plaster of Paris and mounted for support in a hole in fiberboard.

(e), (f), (g) and (h) Analogue two-sided negative stained images taken close to 2-fold directions. (e) and (f): radiographs of (d) taken in very slightly different orientations close to the same 2-fold axis. (g) and (h): radiographs of the same model (d) along two other 2-fold axes.

(i) Analogue image viewed down 3-fold axis.

(j) and (k) Analogue images taken close to the same 5-fold axis of the model.

(l), (m) and (n) Electron micrographs of negatively stained particles of turnip yellow mosaic virus (Finch & Klug, 1966) showing 2-, 3- and 5-fold views, respectively.

The seven analogue images are not all reproduced at exactly the same scale. The small black dots and lines correspond to patches of barium stain used to mark the orientation of the plaster-encased model.

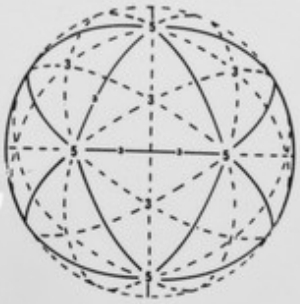

(a)

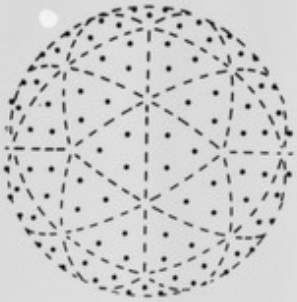

(b)

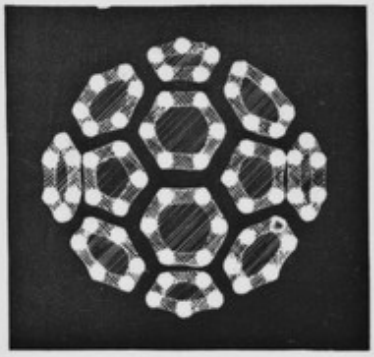

(c)

(d)

(e)

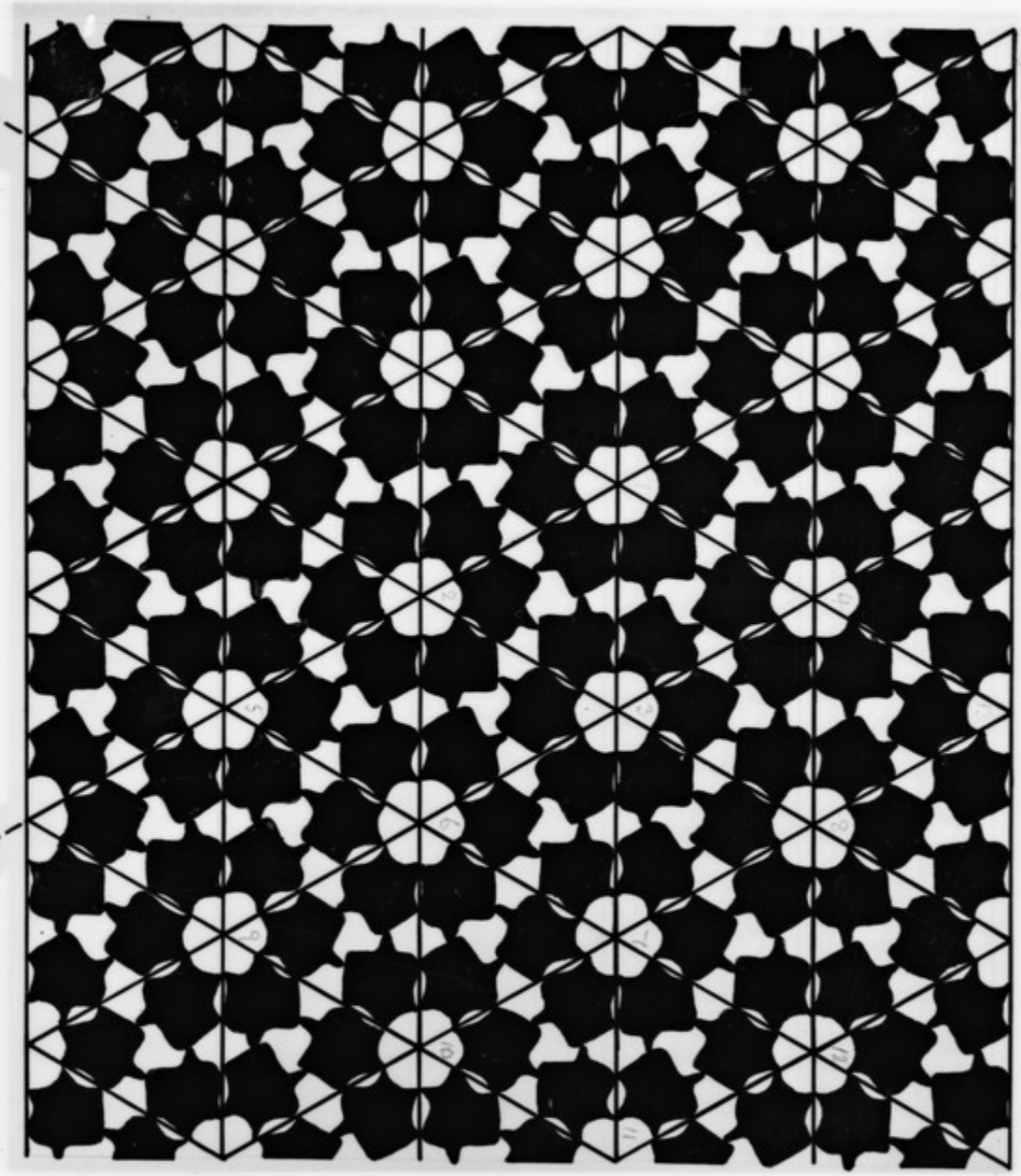

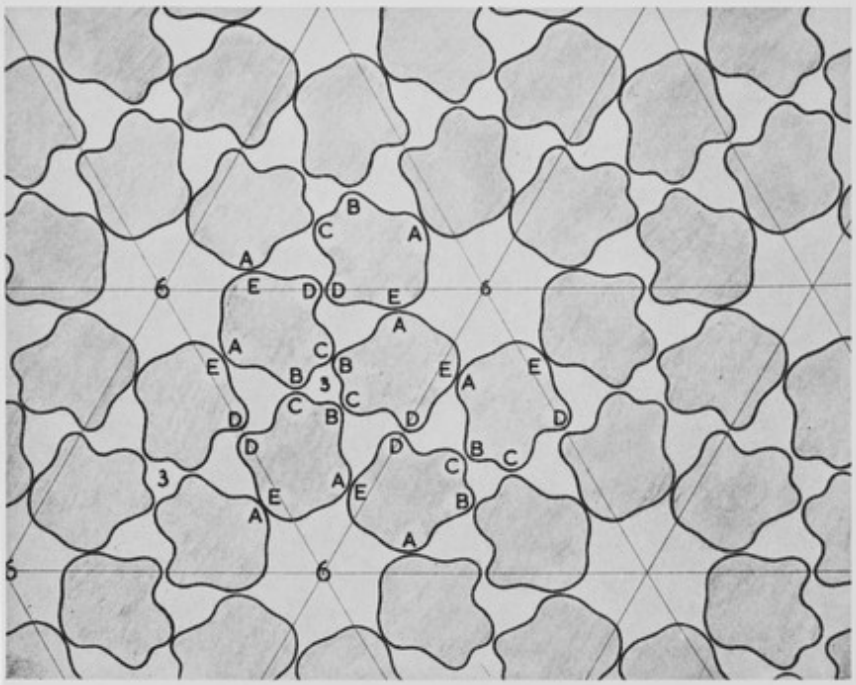

. Asymmetric units arrayed in an equilateral-triangular plane net. Besides having translations, here a and a, the lattice has 6-fold rotational axes of symmetry. Although the asymmetric units are in 6 different orientations in space, they are all exactly equivalently related.

Each unit here is equipped with five "bond" sites, A, B, C, D, and E, forming three different "bonds", namely a hexamer bond AE, a trimer bond BC, and a dimer bond DD. (Note that only two of these bonds are absolutely essential for coherence of the array.)

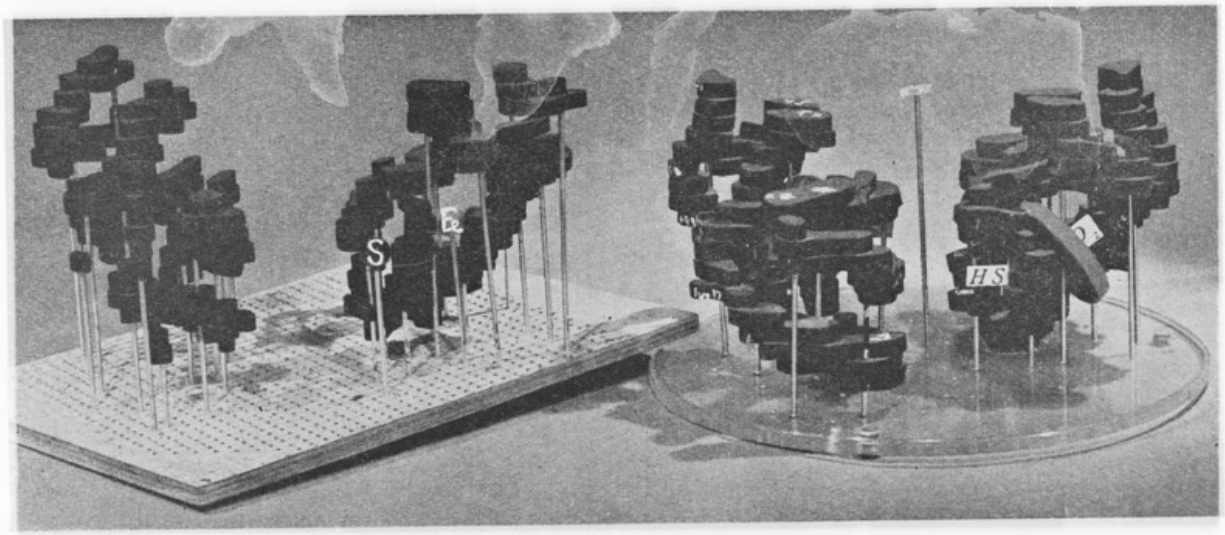

View of the two pairs of β-chains, showing the widening of the gap between them in the human reduced form (left), as compared with horse oxyhæmoglobin (right). The hæm groups in human reduced hæmoglobin are indicated by balls, those in horse oxyhæmoglobin by grey disks. *S* marks one of the mercury atoms of PCMB

per on hæmoglobin H (see p. 639), which shows no hæm–
em interaction and appears to have the same crystal
ructure in the oxygenated and reduced states[12]. This

kinetics of inhibition suggest that these enzymes possess
at least two different active sites, one for combining
with the substrate and another for combining with the
sites
tes in
are indications of structural changes
in these and other enzyme systems[25].

rommel and Bijvoet, 1954), and so the
d the α-carbon atom in optically active
bt. Fig. 10.10 shows this arrangement in

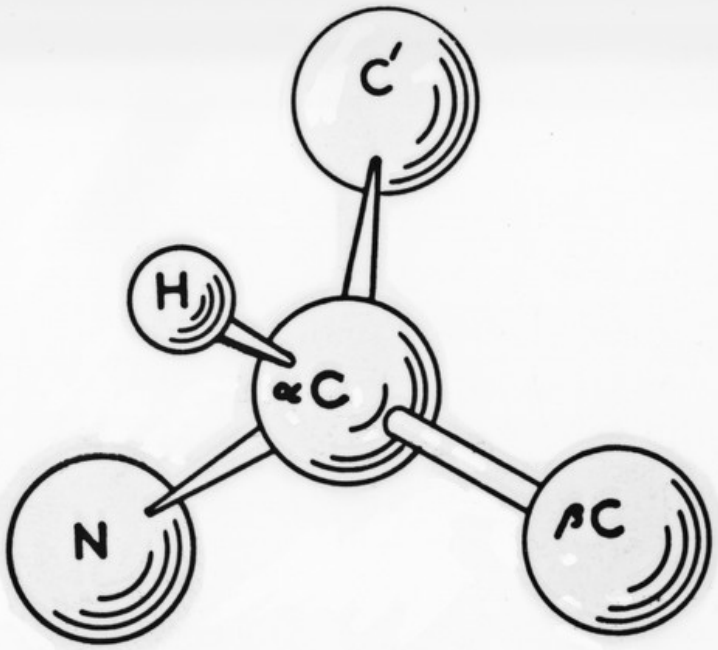

oups
acid
4).

Rotation of Peptides

number of peptides derived from optically

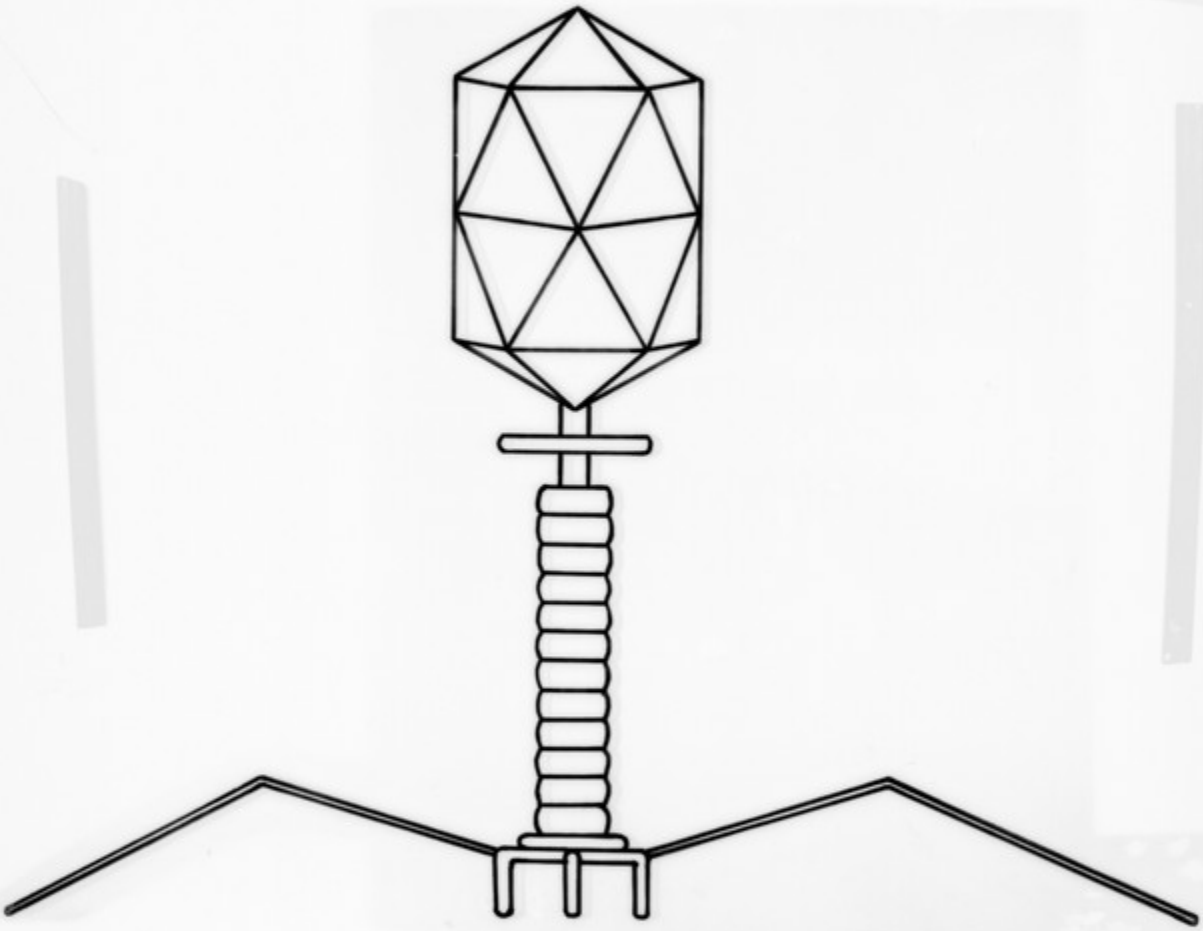

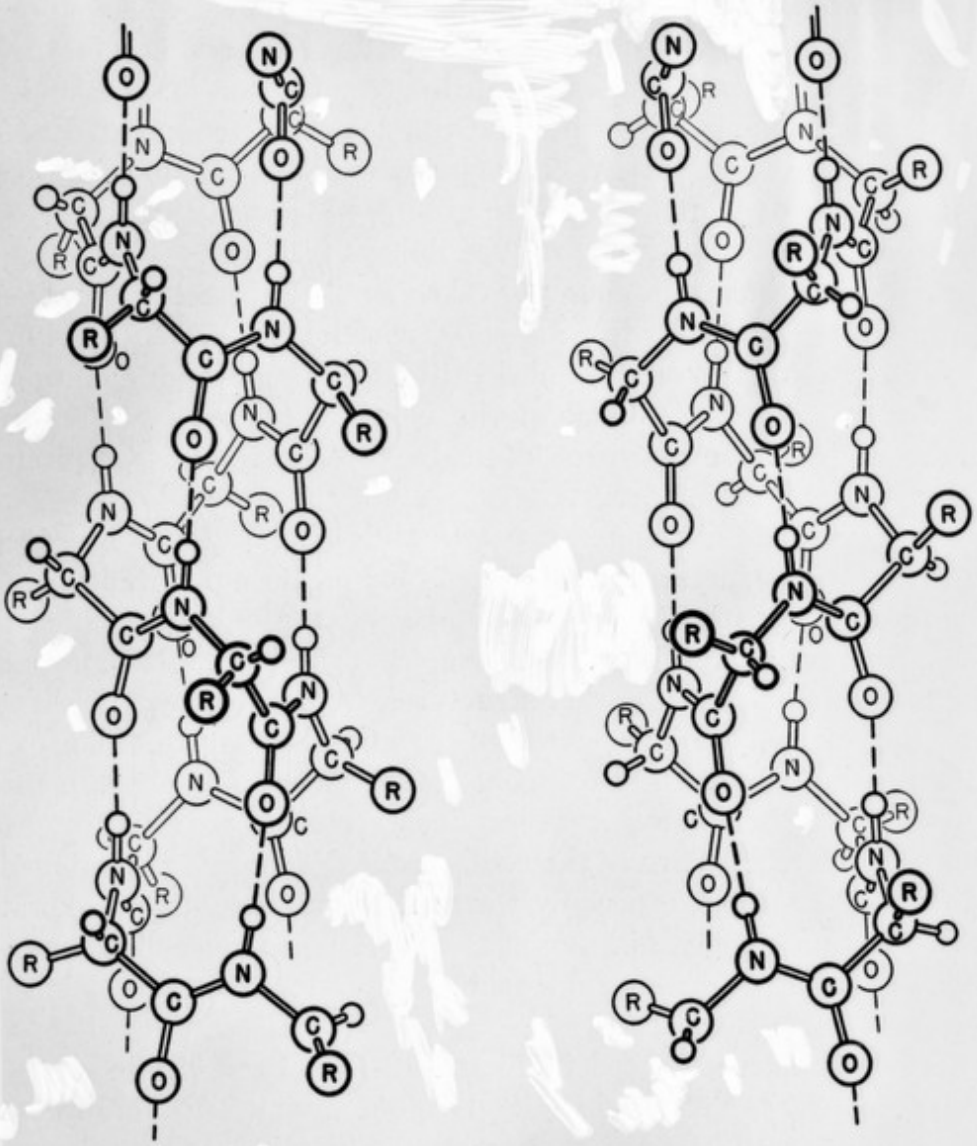

FIG. 12-18.—A drawing showing two possible forms of the alpha helix; the one on the left is a left-handed helix, and the one on the right is a right-handed helix. The amino acid residues have the L-configuration in each case.

it is 6.5 Å for the parallel-chain pleated sheet and 7.0 Å for the antiparallel-chain pleated sheet. Silk fibroin and synthetic poly-*L*-alanine have been found to have the antiparallel-chain pleated-sheet structure.[115] It is likely that the β-keratin structure (assumed by the α-keratin proteins when they are stretched) is that of the parallel-chain

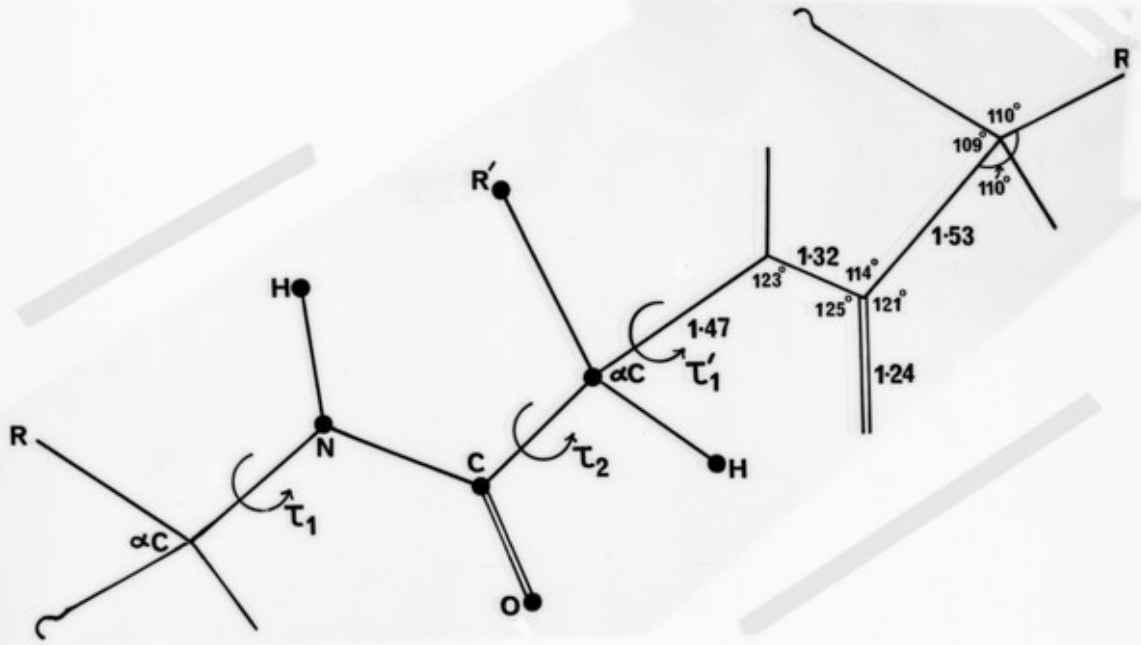
R
110°
109°
110°
R′
1·53
1·32
123°
114°
125°
121°
H
1·47
αC
τ′1
1·24
R
N
C
τ2
H
αC
τ1
O

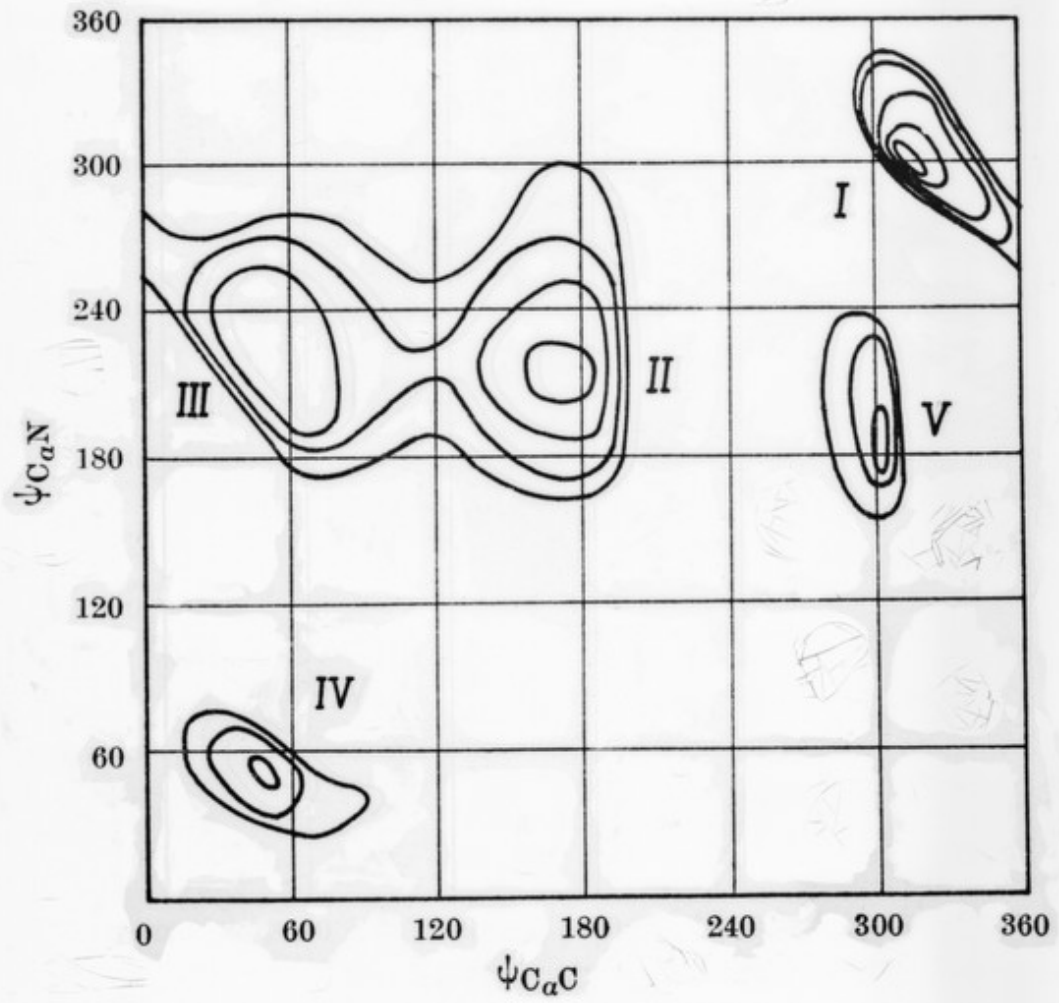

Fig. 2. Two-dimensional plot of the van der Waals conformational potential energy of a chain of poly-L-α-alanine as a function of the angles of rotation $\psi_{C\alpha-C}$ and $\psi_{C\alpha-N}$ about the non-rigid skeleton bonds of the amino-acid residue. Contour lines are drawn at intervals of 1 kcal

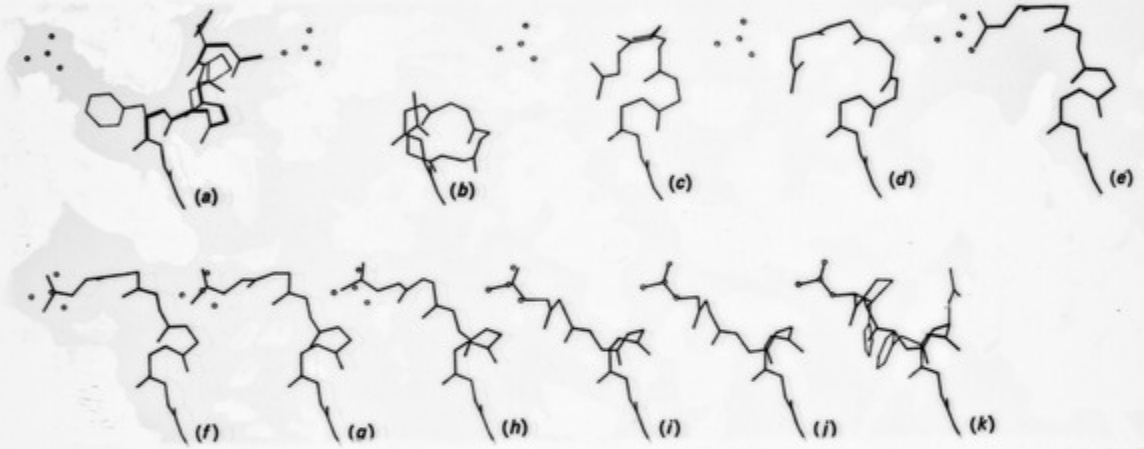

Fig. 4. Cycle by cycle record of the conformations adopted by a length of chain which is required to refold itself so that the free end of the chain comes into coincidence with the guide points shown as open circles on the left of each diagram. There are two peptides at the foot of each figure which do not move; they were guided into those positions and their positions were finalized just before this stage of the calculation was reached. The initial conformation shown in (*a*) is α-helical. The side chains were carried throughout the calculation, but for clarity are shown in only the first and last figures.

diameter of the pa[redacted] studies to be 280 Å, the tips of the mo[redacted]bout 150 Å, and the valleys between at a radius of 130 Å. These relative dimensions were used in building the cork model shown in Plate I(b), and in the drawing in Fig. 2.

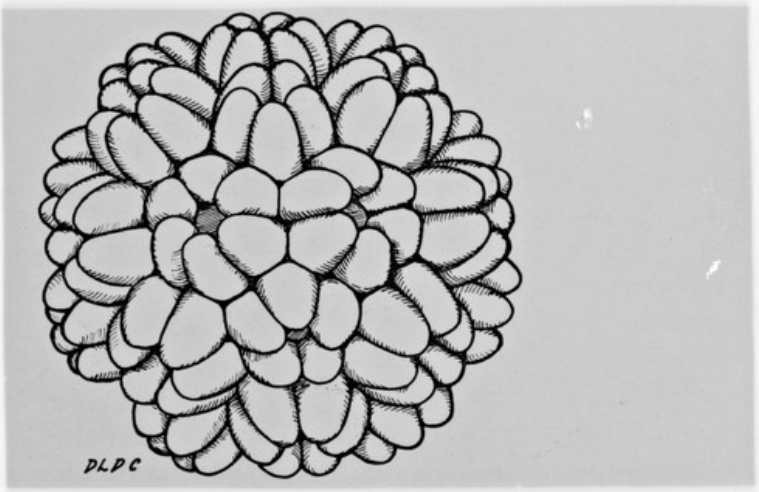

FIG. 2. A drawing of the outer surface of the TYMV particle as revealed by negative staining (approximately ×2 million).

The 180 structure units protrude about 20 Å from the main body of the particle, but their exact shape is not known. They are tilted somewhat out of the radial direction towards the directions of the 3- and 5-fold axes of the particle (although the clustering is not obvious in end-on views in negative-stain images, because the centres of contrast of the units lie below the outermost surface).

The RNA is associated closely with the hexamers and pentamers at an inner radius (see Fig. 4(b) of Part I (Klug *et al.*, 1966)).

Having proceeded so far in our mapping of the surface of the virus particle, it would be reassuring to know that the negative staining of a particle with a shape like that of our model would in fact produce the details in the images that we observe and have used in our deductions of the structure. We are indebted to Dr D. L. D. Caspar for